Concentration of Er^{3+} ions contributing to 1.5-μm emission in Si/Si:Er nanolayers

N. Q. Vinh,[1,2] S. Minissale,[1] H. Vrielinck,[3] and T. Gregorkiewicz[1]

[1]*Van der Waals-Zeeman Institute, University of Amsterdam, Valckenierstraat 65, NL-1018 XE Amsterdam, The Netherlands*

[2]*FOM Institute for Plasma Physics "Rijnhuizen," P.O. Box 1207, NL-3430 BE Nieuwegein, The Netherlands*

[3]*Department of Solid State Sciences, Ghent University, Krijgslaan 281-S1, B-9000 Gent, Belgium*

(Received 3 October 2006; revised manuscript received 21 December 2006; published 24 August 2007)

We have investigated the percentage of Er^{3+} ions which contribute to the low temperature 1.5-μm photoluminescence in Si/Si:Er nanolayer structures grown by sublimation molecular beam epitaxy. In a structure optimized for preferential formation of the Er-1 center with ultranarrow emission lines, we find that emission saturates when approximately 2% of all the Er dopants recombine radiatively upon optical excitation. In a structure where the silicon spacer thickness has been optimized for the maximum (broadband) emission intensity relative to Er contents, we show that in saturation approximately 15% of Er dopants contribute photons. At the same time, from the initial growth of emission intensity on excitation flux at low power, we estimate the maximum percentage of Er ions attaining optical activity. These limits of optical activity of Er in Si/Si:Er nanolayer structures are determined as 25% and 48% for Er-1 and total emission, respectively. In the context of this high level of optical activity, potential of Si/Si:Er nanolayer structures for realization of optical amplification at low temperatures is pointed out.

DOI: 10.1103/PhysRevB.76.085339 PACS number(s): 68.55.Ln, 78.67.Pt, 78.55.Ap, 81.15.Hi

I. INTRODUCTION

While crystalline silicon (*c*-Si) continues to dominate the mainstream integrated circuit device manufacturing, applications of this most important semiconductor material remain electronic rather than photonic. Due to the relatively small and indirect band gap, silicon is a poor light emitter. Nevertheless, as result of continued research effort, optical gain (Si nanocrystals)[1] and Raman lasing (Si)[2] have recently been demonstrated, and even intense room-temperature emission[3] from Si structures seems to be possible. Optical properties of silicon can be enhanced by Er doping but here the situation is still not settled. While room-temperature luminescence has been realized,[4] population inversion and optical gain have not been obtained and fundamental problems remain. Due to the long radiative lifetime of Er^{3+} in Si, a high doping concentration, in the range of $10^{19}-10^{20}$ cm^{-3}, is necessary for intense emission. Such high impurity levels exceed by far the solubility limit and can only be realized by nonequilibrium methods. This readily leads to segregation of Er to the surface and/or in a form of metallic clusters. Although this can be suppressed by oxygen codoping, only a minor part ($\sim$0.1%–1%) of the Er ions incorporated in the material takes part in photon emission.[5,6] This low percentage of Er^{3+} ions which participate in radiative recombination process practically precludes realization of optical gain in Si:Er.

It is generally recognized that for an efficient optical excitation of Er in Si, a high exciton concentration is necessary. This can be obtained in intrinsic material of high purity. Therefore, the requirements of high Er concentration and efficient exciton generation cannot be met simultaneously. This leads to a situation that for heavily Er-doped layers excitons develop in the substrate rather than in the layer itself. Consequently, the intensity of Er-related photoluminescence (PL) does not increase above a certain thickness of the Si:Er layer. This limitation can be overcome when a "spacer" layer of undoped Si is inserted into the Si:Er layer. While thermal stability of Er-related PL is not improved, it turns out that at cryogenic temperatures a sandwich structure of interchanged Si/Si:Er nanolayers features more intense emission at 1.5 μm.[7] In addition, as evidenced by our recent studies, Si/Si:Er nanolayer structures offer a unique possibility of preferential formation of a particular type of optically active Er-related center, labeled Er-1.[8,9] Since the homogeneous emission bands of the Er-1 center are characterized at low temperature by ultrasmall width of a few μeV, this indicates a potential increase of the gain coefficient by a factor of 10^3-10^4 when compared to Si:Er materials used so far. Therefore, Si/Si:Er nanolayers emerge as a promising medium for achieving population inversion and stimulated emission in a Si-based material, while in view of thermal quenching of PL emission this could possibly be obtained at cryogenic temperatures only (at this point), it would nevertheless represent a major advance, as realization of population inversion and optical gain is a long sought after goal of silicon science and technology. A necessary (although by itself insufficient) condition for that is a very high percentage of dopants which can participate in radiative recombination. In this paper, we investigate the limits of optical activity of Er in Si/Si:Er nanolayer structures, i.e., the maximum concentration of Er dopants which contribute photons upon optical excitation.

II. SAMPLE PREPARATION AND EXPERIMENT

All the measurements presented in this paper have been performed at cryogenic temperatures (4–15 K) in two specific, differently optimized Si/Si:Er nanolayer structures grown by sublimation molecular beam epitaxy (SMBE) at 560 °C. Both of these structures comprise interchanged Si and Si:Er layers stacked along the ⟨100⟩ growth direction to the total thickness of approximately 1 μm. Er concentration in the doped regions was determined by secondary ion mass spectrometry as 3.5×10^{18} cm^{-3}. Past results show that emis-

 ©2007 The American Physical Society

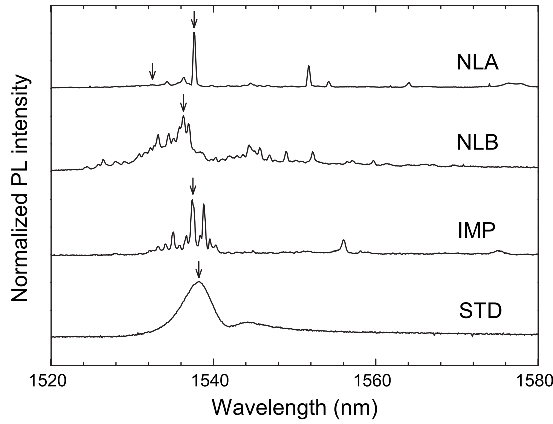

FIG. 1. PL spectra of the samples used in the present study: SMBE-grown nanolayer structures NLA and NLB, Er-implanted sample IMP, and the SiO_2:Er "standard" STD under cw excitation, λ_{exc}=488 nm. The arrows indicate spectral points where the PL intensity power dependence has been measured (Fig. 2).

sion from Si/Si:Er nanolayer structures depends strongly on the thickness of Si:Er doped layers and Si spacers. The two structures used in this study have been differently optimized. The first one, labeled NLA, was optimized for preferential formation of the Er-1 center. Its PL spectrum—see Fig. 1—contains almost exclusively the ultrasharp lines characteristic for that center. In the second structure, NLB, the ratio between active volume and spacer thickness has been optimized for the maximum total PL intensity of the (broad) 1.5-μm band. In sample NLA, the Si:Er nanolayers of 2.3 nm are separated by 1.7 nm thin spacers of undoped Si. Following the growth procedure, the structure was annealed at 800 °C for 30 min. In sample NLB, the ~5 nm doped layers are separated by much thicker Si spacers of ~100 nm. This sample is characterized by an inhomogeneously broadened 1.5-μm band. The total Er areal densities are 2×10^{14} and 2×10^{13} cm^{-2} for structures NLA and NLB, respectively. In order to quantify the intensity of the Er-related emission from multinanolayers, a SiO_2:Er "standard" sample, labeled further STD, was used. This has been prepared by a triple Er implantation (1.5×10^{14} cm^{-2} at 200 keV, 2.8×10^{14} cm^{-2} at 500 keV, and 5.6×10^{14} cm^{-2} at 1000 keV) to the total dose of 9.9×10^{14} cm^{-2}, and subsequent 30 min annealing at 1000 °C in nitrogen gas. These conditions have been chosen in order to achieve the full optical activation of all Er dopants and minimize nonradiative recombination.[10,11] The latter has been checked by measuring the decay time of Er emission; this was found to be $\tau_{SiO_2:Er}\approx13$ ms, which indeed corresponds to the reported radiative lifetime of 1.5-μm Er PL in SiO_2.[11,12] For reference, in order to validate the experimental method used for determination of the percentage of optically active Er, an implanted Si:Er sample labeled IMP was used. This sample is representative for state-of-the-art Si:Er material which can be obtained by implantation. It has been prepared by Er implantation (3×10^{12} cm^{-2}, 300 keV) and oxygen (3×10^{13} cm^{-2}, 40 keV) coimplantation followed by 30 min 900 °C annealing, with these preparation conditions being optimized for the maximum emission intensity.[13]

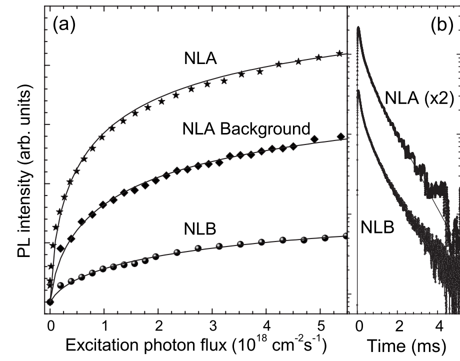

FIG. 2. Excitation power dependence under cw excitation, λ_{exc}=514.5 nm (a), and decay dynamics under pulsed excitation, λ_{exc}=520 nm (b) of Er-related PL for the SMBE-grown structures NLA and NLB.

The PL experiments were carried out at liquid-He temperatures in a continuous-flow cryostat (Oxford Instruments Optistat CF). The samples were excited using an Ar^+-ion laser or a tunable optical parametric oscillator (OPO) producing pulses of 5 ns duration at 20 Hz repetition rate. The luminescence was resolved with a 1 m F/8 monochromator (Jobin-Yvon THR-1000) equipped with a 900 grooves/mm grating blazed at 1.5 μm and detected by an infrared photomultiplier with a 30 μs response time.

III. RESULTS AND DISCUSSION

Figure 1 shows (normalized) the PL spectra of the four samples used in the present study. These were obtained at T=4.2 K, outside the saturation range under continuous wave (cw) excitation with an Ar^+-ion laser operating at 488 nm. For sample NLA, the characteristic ultranarrow lines of the Er-1 center can easily be distinguished.[9] Some sharp lines can also be found in the broad spectrum of sample NLB. The integrated PL spectrum intensity ratio for all the samples, normalized to the same signal maximum, and thus reflecting only different spectral characteristics, is

$$I_{NLA}:I_{NLB}:I_{IMP}:I_{STD}=1:5.6:2.5:4. \quad (1)$$

The excitation power dependence of the PL intensity for samples NLA and NLB under cw excitation at λ_{exc} =514.5 nm was measured at 4.2 K. The emission wavelengths selected for this experiment are indicated by arrows in Fig. 1. Figure 2(a) shows the power dependence of the PL intensity for the main line at λ=1537.8 nm and at a wavelength of λ=1532.5 nm for the "background" feature for sample NLA, and λ=1536.3 nm for sample NLB. As has been discussed previously,[14,15] under cw excitation conditions, the power dependence of Si:Er PL intensity is well described with the formula:

$$I_{PL}=\frac{A\sigma\tau\Phi}{1+\beta\sqrt{\sigma\tau\Phi}+\sigma\tau\Phi}, \quad (2)$$

where σ is an effective excitation cross section of Er^{3+} ion, τ is the effective lifetime of Er^{3+} in the excited state, and Φ is

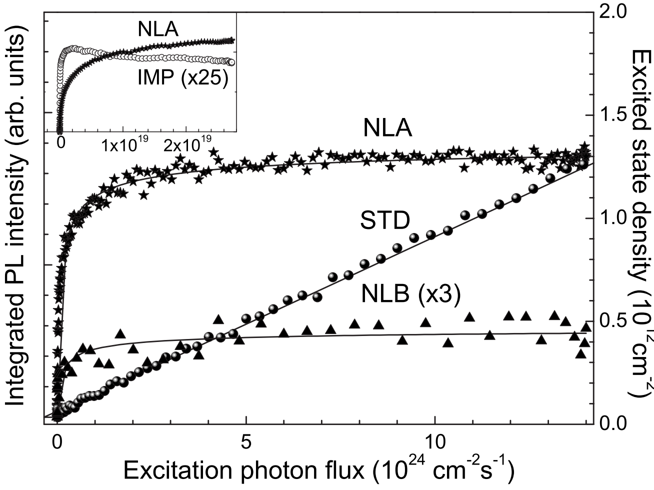

FIG. 3. Comparison of PL intensity of SMBE-grown structures NLA and NLB with the SiO_2:Er "standard" STD sample in saturation under pulsed excitation, $\lambda_{exc}=520$ nm. In the inset, power dependencies of samples NLA and IMP are compared.

the flux of photons. The appearance of the $\beta\sqrt{\sigma\tau\Phi}$ term, with an adjustable parameter β, is a fingerprint of the Auger effect hindering the luminescence. The solid curves in Fig. 2(a) represent the best fits to the experimental data using Eq. (2). For sample NLA, we get $\sigma_{cw}^{NLA}=5\pm2\times10^{-15}$ cm^2 (identical) for the Er-1 related lines and an order of magnitude smaller value of $\sigma_{cw}^{bkg}=7.5\pm2\times10^{-16}$ cm^2 for the background emission, with the Auger process related parameter $\beta=2\pm0.1$. For sample NLB, the best fit is obtained for $\sigma_{cw}^{NLB}=2\pm1\times10^{-15}$ cm^2 and $\beta=2\pm0.1$. The values of σ are similar to those reported for Er-implanted silicon[16] and indicate a similar Er excitation mechanism.

Figure 2(b) shows the decay characteristics of Er-related PL at $T=4.2$ K under pulsed excitation with a wavelength of $\lambda_{exc}=520$ nm. As can be seen, the decay kinetics is composed of a fast and a slow component. Fitting the profiles measured for sample NLA, we obtained two decay times of $\tau_F=0.16$ ms and $\tau_S=0.83$ ms contributing to the relaxation. The intensity ratio of the fast and slow components is found to be 3:2, the same for all the emission lines of this sample. For sample NLB, we have $\tau_F=0.19$ ms and $\tau_S=0.90$ ms. These values are again similar to those commonly found in Si:Er structures prepared by implantation.[16] (For IMP, we get $\tau_{IMP}=1.9$ ms.)

As mentioned before, the percentage of Er dopants that can emit photons upon excitation is known to be notoriously low in Si,[17] dispersions of Si nanocrystals in SiO_2,[18] and also in other semiconductors matrices, e.g., GaN. Yet, this parameter is crucially important for the application potential of Er-doped semiconductors and, in particular, for Si:Er, since it determines the PL intensity and is decisive for (a possibility of achieving) population inversion. An estimate of the number of excitable centers can be made by comparing the intensity of the observed PL with that of the SiO_2:Er standard STD sample measured under the same conditions. This is presented in Fig. 3, where flux dependencies of Er-related PL intensities are shown for samples NLA, NLB, and STD. The experiment has been performed under pulsed excitation with the OPO set to $\lambda_{exc}=520$ nm. This particular wavelength corresponds to the ${}^4I_{15/2}\rightarrow{}^2H_{11/2}$ internal transition of Er^{3+} ion and therefore can be used for both indirect (Si) and direct (SiO_2) excitations of Er^{3+} ions. Since, in the experiment, the PL signal is effectively integrated over time, and the PL intensity is proportional to N_{Er}^*/τ_{rad}, the result of the experiment is given by $N_{Er}^*\tau/\tau_{rad}$. Therefore, the ratio of the number of photons emitted from the two investigated samples after an excitation pulse is given by

$$\frac{I_{Si:Er}}{I_{SiO_2:Er}}=\frac{\eta_{out}^{Si}}{\eta_{out}^{SiO_2}}\frac{N_{Er(Si:Er)}^*\times(\tau_1/\tau_1^{rad})}{N_{Er(SiO_2:Er)}^*\times(\tau_2/\tau_2^{rad})}, \quad (3)$$

where τ_1, τ_2, τ_1^{rad},τ_2^{rad}, $N_{Er(Si:Er)}^*$, $N_{(SiO_2:Er)}^*$, η_{out}^{Si}, $\eta_{out}^{SiO_2}$ are the effective and radiative decay times, density of excited Er^{3+} ions, and the fraction of emitted photons that leave the sample (extraction efficiency), respectively, for the Si:Er and SiO_2:Er materials. The ratio of the extraction efficiencies can be calculated from the refractive indices of Si and SiO_2:

$$\frac{\eta_{out}^{Si}}{\eta_{out}^{SiO_2}}=\frac{\frac{1}{4}\times\frac{n_{air}^2}{n_1^2}}{\frac{1}{4}\times\frac{n_{air}^2}{n_2^2}}\simeq0.175, \quad (4)$$

where n_1, n_2 are the reflective indices of 3.49 and 1.46 at 1.5-μm emission for Si and SiO_2, respectively.[19,20]

In the present experiment, the duration of the OPO pulse ($\Delta t=5$ ns) is much shorter than the characteristic lifetime τ of Er^{3+} in the excited state: $\Delta t\ll\tau$. Consequently, we can assume that recombination does not take place during illumination, and the population N_{Er}^* reaches the level of

$$N_{Er}^*(t=\Delta t)=N_{Er}^{ex}[1-\exp(-\sigma\Phi\Delta t)]. \quad (5)$$

In this equation, N_{Er}^{ex} is the total concentration of excitable Er^{3+} ions present in the sample. For low excitation density, when $\sigma\Phi\Delta t\ll1$, this formula gives a linear dependence on flux: $N_{Er}^*=\sigma\Phi N_{Er}^{ex}\Delta t$. When $\sigma\Phi\Delta t\gg1$, the saturation regime can be obtained: $N_{Er}^*=N_{Er}^{ex}$. From Fig. 3, we conclude that the intensity of emission from SiO_2:Er sample shows a linear dependence over the whole investigated flux range. For the SiO_2:Er system, the values of all parameters are known: $\sigma_{SiO_2:Er}^{520\text{ nm}}=2\times10^{-20}$ cm^2,[10] and $N_{Er}^{ex}=9.9\times10^{14}$ cm^{-2}, i.e., we assume that all the implanted ions participate in emission. We also take $\tau/\tau_{rad}=1$. In that way, the well-characterized SiO_2:Er system can be used to attribute the measured PL intensity to a particular areal density (cm^{-2}) of excited Er^{3+} ions, as given by the right hand scale in Fig. 3.

For Si, the Er^{3+} excited state population should be corrected due to the nonradiative contribution to the effective lifetime.[21] If we assume the slow component in the decay kinetic to represent radiative recombination (which seems very reasonable in view of the published data on the radiative decay of Er in *c*-Si[16]), the correction to the integrated PL intensities is given by

$$\frac{I_{\text{Si:Er}}}{I_{\text{Si:Er (total)}}} = \frac{N_{\text{Er}}^{*}\tau/\tau_{\text{rad}}}{N_{\text{Er}}^{*}\tau_{\text{rad}}/\tau_{\text{rad}}} = \frac{\tau}{\tau_{\text{rad}}} = \frac{A_F\tau_F + A_S\tau_S}{(A_F+A_S)\tau_S} = \frac{A_F/A_S\tau_F + \tau_S}{(A_F/A_S+1)\tau_S}, \quad (6)$$

where A_F, A_S, τ_F, τ_S correspond to the amplitudes and decay times of the fast and the slow components of the signal, respectively. At the saturation level of the sample NLA, $A_F/A_S=1.5$, $\tau_F=0.16$ ms, $\tau_S=0.83$ ms, and we get $I_{\text{Si:Er}}/I_{\text{total}}=\tau/\tau_{\text{rad}}\approx 0.5$. Therefore, under the same excitation conditions, the excited state population in this sample has to be two times higher in order to give PL intensity equal to that of sample SiO_2:Er. This is similar for the sample NLB, for which we get $\tau/\tau_{\text{rad}}\approx 0.45$. Using data of Fig. 3, the maximum number of Er^{3+} ions emitting photons in the Si:Er samples can be derived from the saturation level of PL intensity, and taking into account the different spectral shape of the 1.5-μm band [Eq. (1)], effective lifetime, and extraction loss. For sample NLA, we have $N_{\text{Er}}^{\text{ex}}\approx 1.4\times 10^{12} \times (1/0.175)\times 2\times (1/4)=4.0\times 10^{12}$ cm^{-2}. This implies that at saturation the percentage of Er dopants contributing to photon emission is $P_{\text{NLA}}\approx 2\pm 0.5\%$. For sample NLB, with a lower signal-to-noise ratio, we arrive at $N_{\text{Er}}^{\text{ex}}\approx 0.17\times 10^{12} \times (1/0.175)\times (1/0.45)\times (5.6/4)=3.0\times 10^{12}$ cm^{-2} and $P_{\text{NLB}} \approx 15\pm 5\%$.

To cross-check the methodology, we performed a comparative measurement using the implanted sample IMP. In the inset of Fig. 3, the power dependence of PL intensity is shown for samples NLA and IMP. The experiment has been performed at low temperature under cw Ar laser excitation. As can be seen, the PL saturation intensity of sample NLA is about 25–30 times larger than that of IMP. Based on that, and taking into account the difference in effective decay time ($\times 2$) and spectral shape, we obtain in this case the percentage of radiatively recombining Er dopants as $P_{\text{IMP}} \approx 6.6\pm 1\%$. This value is in reasonable agreement with the optical activation limit of state-of-the-art *c*-Si:Er codoped with oxygen[11] and provides verification of the method and approximations used in this work.

We note that the percentage of photon-emitting Er dopants obtained for the Si/Si:Er multinanolayer structure NLA from PL saturation level is comparable to that achieved in the best Si:Er materials prepared by ion implantation. We point out that in view of the relatively long radiative lifetime of Er in Si τ_{rad} used here for concentration evaluation, the estimated percentage should be seen as the lower limit.

Alternatively, the amount of Er^{3+} ions participating in the radiative recombination can be estimated from the linear part of the excitation power dependence under pulsed excitation. Such an approach seems more appropriate, since the simple excitation model used here does not take into account various cooperative processes which are important in the saturation regime. The linear part of integrated PL intensity, determined as the number of photons emitted after each laser pulse, is given by

$$I_{\text{Si:Er}} = \sigma_{\text{Si:Er}}\alpha\Phi N_{\text{Si:Er}}^{\text{ex}}\Delta t\frac{\tau}{\tau_{\text{rad}}},$$

and

$$I_{\text{SiO}_2\text{:Er}} = \sigma_{\text{SiO}_2\text{:Er}}^{520\text{ nm}}\Phi N_{\text{SiO}_2\text{:Er}}^{\text{ex}}\Delta t\frac{\tau}{\tau_{\text{rad}}}, \quad (7)$$

for the Si:Er and SiO_2:Er samples, respectively. The correction factor α indicates photon loss due to the surface reflection of Si. For a Si-air interface at normal incidence, this can be estimated as $\alpha=70\%$.[22] Reflection loss for SiO_2 is negligible. The linear component for samples NLA and NLB is taken as a derivative for photon flux $\Phi\approx 0$ of the fitting curves depicted in Fig. 3. These values are scaled with the linear dependence found for the SiO_2:Er standard sample STD. When corrected for the shape of individual spectra, the lifetime, and with the average excitation cross section as determined earlier and now scaled for Si absorption at 520 nm, we can estimate the upper limit of the total concentration of excitable Er^{3+} ions $[N_{\text{Er}}^{\text{ex}}]_{\text{max}}$. In that way, we get the $[N_{\text{Er}}^{\text{ex}}]_{\text{max}}$ values of $25\pm 10\%$ and $48\pm 20\%$ for samples NLA and NLB, respectively. It is important to point out that these values correspond to an idealization when no effects related to the increased concentration of Er in the excited state is taken into account. Nevertheless, they are of importance as being indications to the upper limit of Er activation.

IV. CONCLUSIONS

Based on the presented results, we conclude that the percentage of Er dopants undergoing radiative recombination and contributing to the 1.5-μm emission in SMBE-grown Si nanolayers is similar to that realized in the best Si:Er structures prepared by ion implantation. However, in contrast to the implanted material, all the Er emitters in the NLA structure are incorporated in a single type of optical center, resulting in the ultranarrow homogeneous linewidth of PL bands. Moreover, the already relatively high percentage of emitting Er^{3+} ions as found for the Si/Si:Er nanolayer structure NLA can possibly be further improved. This prospect is justified by the results obtained for sample NLB, for which our estimate gives the active Er fraction in excess of 10%, with the upper limit being comparable with the total Er contents. Future research will tell whether also for such a structure an appropriate thermal treatment can preferentially convert emitting centers into the Er-1, as was the case for NLA. We point out that the calculated high percentage of Er dopants which contribute to the 1.5-μm emission in Si/Si:Er nanostructures corresponds to the absolute concentration which is similar to the solid solubility limit of Er in crystalline Si.[23] The high percentage of emitting dopants combined with the ultranarrow emission lines makes the Si/Si:Er multinanolayers materials interesting for silicon photonics. In particular, the Si/Si:Er nanolayer structures appear promising for realization of population inversion and, consequently, optical amplification at low temperature. Investigations which aim at clarification of this essential point are currently on the way.

ACKNOWLEDGMENTS

The authors gratefully acknowledge F. W. Widdershoven for preparation of the STD sample used for calibration. The SMBE-grown structures NLA and NLB were kindly provided by Z. Krasil'nik, and the implanted sample IMP by W. Jantsch. Henk Vrielinck acknowledges a financial support of the Research Foundation-Flanders (FWO Vlaanderen). This work is part of the research program of FOM, which is financially supported by NWO.

[1] L. Pavesi, L. Dal Negro, C. Mazzoleni, G. Franzó, and F. Priolo, Nature (London) **408**, 440 (2000).
[2] H. Rong, A. Liu, R. Jones, O. Cohen, D. Hak, R. Nicolaescu, A. Fang, and M. Paniccia, Nature (London) **433**, 292 (2005).
[3] W. L. Ng, M. A. Lourenço, R. M. Gwilliam, S. Ledain, G. Shao, and K. P. Homewood, Nature (London) **410**, 192 (2001).
[4] G. Franzó, F. Priolo, S. Coffa, A. Polman, and A. Carnera, Appl. Phys. Lett. **64**, 2235 (1994).
[5] S. Coffa, G. Franzó, F. Priolo, A. Polman, and R. Serna, Phys. Rev. B **49**, 16313 (1993).
[6] G. N. van den Hoven, J. H. Shin, A. Polman, S. Lombardo, and S. U. Campisano, J. Appl. Phys. **78**, 2642 (1995).
[7] B. A. Andreev, A. Yu. Andreev, H. Ellmer, H. Hutter, Z. F. Krasil'nik, V. P. Kuznetsov, S. Lanzerstorfer, L. Palmetshofer, K. Piplits, R. A. Rubtsova, N. S. Sokolov, V. B. Shmagin, M. V. Stepikhova, and E. A. Uskova, J. Cryst. Growth **201/202**, 534 (1999); M. V. Stepikhova, B. A. Andreev, V. B. Shmagin, Z. F. Krasil'nik, V. P. Kuznetsov, V. G. Shengurov, S. P. Svetlov, W. Jantsch, L. Palmetshofer, and H. Ellmer, Thin Solid Films **369**, 426 (2000).
[8] N. Q. Vinh, H. Przybylińska, Z. F. Krasil'nik, and T. Gregorkiewicz, Phys. Rev. Lett. **90**, 066401 (2003).
[9] N. Q. Vinh, H. Przybylińska, Z. F. Krasil'nik, and T. Gregorkiewicz, Phys. Rev. B **70**, 115332 (2004).
[10] W. J. Miniscalco, J. Lightwave Technol. **9**, 234 (1991).
[11] A. Polman, J. Appl. Phys. **82**, 1 (1997).
[12] A. Polman, D. C. Jacobson, D. J. Engelsham, R. C. Kistler, and J. M. Poate, J. Appl. Phys. **70**, 3778 (1991).
[13] H. Przybylińska, W. Jantsch, Yu. Suprun-Belevitch, M. Stepikhova, L. Palmetshofer, G. Hendorfer, A. Kozanecki, R. J. Wilson, and B. J. Sealy, Phys. Rev. B **54**, 2532 (1996).
[14] J. Palm, F. Gan, B. Zheng, J. Michel, and L. C. Kimerling, Phys. Rev. B **54**, 17603 (1996).
[15] D. T. X. Thao, C. A. J. Ammerlaan, and T. Gregorkiewicz, J. Appl. Phys. **88**, 1443 (2000).
[16] F. Priolo, G. Franzó, S. Coffa, and A. Carnera, Phys. Rev. B **57**, 4443 (2005).
[17] A. Polman, G. N. van den Hoven, J. S. Custer, J. A. Shin, and R. Serna, J. Appl. Phys. **77**, 1256 (1995).
[18] M. Wojdak, M. Klik, M. Forcales, O. B. Gusev, T. Gregorkiewicz, D. Pacifici, G. Franzó, F. Priolo, and F. Iacona, Phys. Rev. B **69**, 233315 (2004).
[19] Pochi Yeh, *Optical Waves in Layered Media* (Wiley, New York, 1988).
[20] A. J. Steckl, J. Heikenfeld, and S. C. Allen, J. Disp. Technol. **1**, 157 (2005).
[21] N. Q. Vinh, S. Minissale, B. A. Andreev, and T. Gregorkiewicz, J. Phys.: Condens. Matter **17**, S2191 (2005).
[22] *Properties of Crystalline Silicon*, edited by Robert Hull (INSPEC, London, 1999).
[23] D. J. Engelsham, J. Michel, E. A. Fitzgerald, D. C. Jacobson, J. M. Poate, J. L. Benton, A. Polman, Y.-H. Xie, and L. C. Kimerling, Appl. Phys. Lett. **58**, 2797 (1991).